6B.8 PREDICTION AND MITIGATION OF ANOMALOUS PROPAGATION WITH THE TOTAL ATMOSPHERIC EFFECTS MITIGATION (TAEM) SYSTEM

James J. Stagliano[1*], J. Clayton Kerce[1], G. Martin Hall[1], Robert D. Bock[1], E. Jeff Holder[1], Susan F. Dugas[1], Francois Vandeburge[2]

[1]Propagation Research Associates, Inc.
[2]National Center for Atmospheric Research

1. INTRODUCTION

Anomalous propagation (AP) impacts the quality of precipitation estimates and many decisions, public safety resource management, and economic, that rely on accurate geolocated precipitation measurements. Techniques to automatically identify and mitigate the effects of AP in the radar data have been developed and implemented in systems such as the Hydrological Decision Support System (HDSS) and the Radar Echo Classifier (REC). These techniques detect AP through its statistical properties in the radar data and remove contaminated data.

The goal of the Total Atmospheric Effects Mitigation (TAEM) system is to predict AP to aid in the mitigation of this artifact in the radar data. TAEM uses atmospheric measurements coupled with a numerical weather prediction (NWP) model to characterize the propagation environment. This characterization is subsequently fed into a propagation model to propagate the radar pulses in the simulated atmosphere. The model uses standard techniques such as the parabolic equation method (PEM) with which to model the propagation of electromagnetic waves in the atmosphere, the model predicts the anomalous propagation for various frequencies and scan configurations, thereby predicting which scan configurations will minimize the AP or alternately where AP may be located.

This paper briefly reviews anomalous propagation, describes the TAEM system and presents preliminary results in predicting AP in the Atlanta, GA area correlated with the Peachtree City, GA WSR-88D.

2. ANOMALOUS PROPAGATION REVIEW

Anomalous propagation, also known as range clutter, occurs when the radar beam is bent down to the earth's surface. This phenomenon results from atmospheric refractivity gradients.

If the atmosphere was homogenous electromagnetic radiation would travel in a straight line. However, the atmosphere is not homogeneous, rather it is stratified, thus the index of refraction, *n*, varies with altitude. For this review, we will use the standard assume horizontal homogeneity, though this assumption is not true in general. Thus, the index of refraction can be considered as layered within the atmosphere as shown in Figure 1. Though the index of refraction varies, its variation is quite small. Therefore, it is standard to transform the index of refraction *n* into *refractivity* units, *N* via the definition,

$$N = (n-1)\times 10^6 \quad . \tag{1}$$

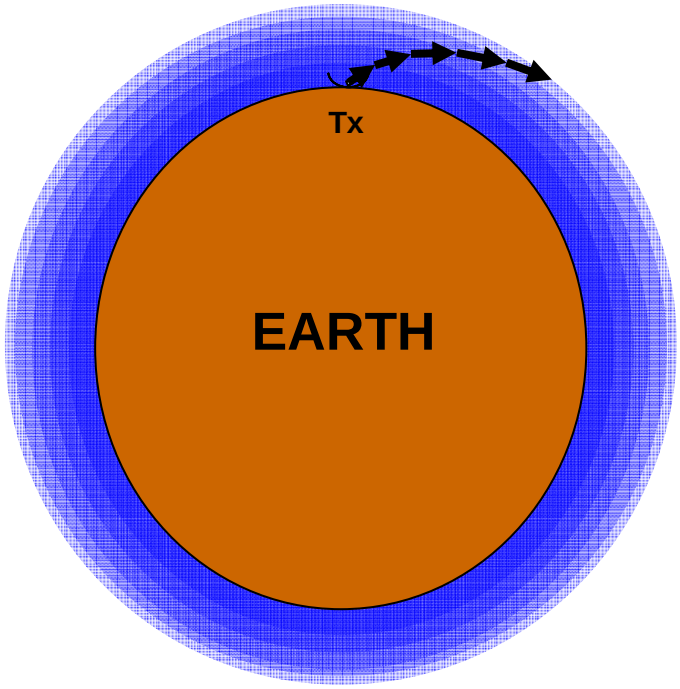

Figure 1 The stratified index of refraction due to the nonhomogeneous atmosphere.

For example, the index of refraction for air at standard temperature, pressure, and humidity is accepted to be n_{air} = 1.000298, its refractivity is N_{air} = 298 N-units.

The associated vertical gradient of refractivity with respect to index of refraction is,

$$\frac{dN}{dh} = \frac{dn}{dh}\times 10^6 \quad . \tag{2}$$

Thus, the variation in refractivity is proportional to the variation in the index of refraction.

Considering a radar scanning at an elevation ϕ. As the ray travels outward through the different layers, it is bent a little as it traverses from one layer to the next. The amount of bending is described by the *curvature*, the change in angle with respect to arclength,

$$C(h) = \frac{d\phi}{ds} = \frac{dn}{dh} \quad . \tag{3}$$

[*]*Corresponding author address*: James. J. Stagliano, Propagation Research Associates, Inc., 1275 Kennestone Circle, Suite 100, Marietta, Ga 30066; e-mail: jim.stagliano@pra-corp.com

The curvature of the ray *with respect to the surface of the* Earth is given by adding this curvature to the reciprocal of the radius of the Earth,

$$C_E(h) = \frac{1}{R_E} + \frac{dn}{dh} \quad . \tag{4}$$

As an example, consider a ray that follows the Earth curvature, i.e. the ray stays at a constant height above the surface of the earth. The curvature with respect to the earth surface is zero, $C_E(h) = 0$ resulting in vertical gradient in the index of refraction of $\frac{dn}{dh} = -1.569 \times 10^{-4} \frac{1}{km}$, which gives the associated refractivity gradient of $\frac{dN}{dh} = -156.9 \frac{N-units}{km}$. Thus when $\frac{dN}{dh} > -156.9 \frac{N-units}{km}$, the ray will bend away from the Earth's surface and out towards space. Similarly, when the gradient is less than -157 N-units/km, the ray will bend down towards the Earth's surface. The refractivity gradient is used to classify the refractive environment into three general types, subrefractive where there is significant bending away from the earth's surface, normal propagation, and superrefraction where the rays bend back towards the earth's surface. This classification is summarized in Table 1 (Battan, 1981) and Figure 2.

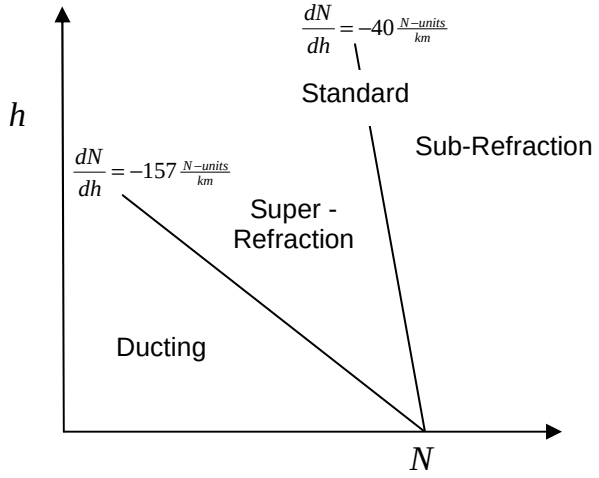

Figure 2 The refractive regimes

It is the latter classification, the ducting environment that causes AP.

A common exercise is to determine the curvature, or actually the reciprocal of the curvature (or effective Earth radius) that results in a straight line path for the electromagnetic pulse for a "standard" atmosphere. The vertical gradient for the standard atmosphere is $\frac{dN}{dh} = -40 \frac{N-units}{km}$ (Battan, 1981), resulting in an effective Earth radius of $R' = 1.34 R_E \approx \frac{4}{3} R_E$. Thus, the standard assumption of the 4/3 Earth radius comes from assuming a standard atmosphere. In reality, the effective Earth radius can vary from 1.1 R_E to 1.6 R_E based upon atmospheric conditions (Rinehart, 1991).

Table 1 Refractive Environment Classification

Vertical Gradient of Refractivity	Refractive Environment
$\frac{dN}{dh} > 0 \frac{N-units}{km}$	Subrefractive
$0 > \frac{dN}{dh} > -156.9 \frac{N-units}{km}$	Super Refraction
$-157 \frac{N-units}{km} > \frac{dN}{dh}$	Ducting

As the AP phenomenon is strongly dependent upon a highly negative gradient in the refractivity, it is natural to review the atmospheric conditions that result in these gradients.

2.1. Atmospheric Conditions associated with AP

The refractivity is dependent upon the atmospheric pressure, temperature, and partial water vapor pressure (Bean, 1966), via

$$N(p,T,e) = a\frac{p}{T} + b\frac{e}{T^2} \quad , \tag{5}$$

where $a = 77.6 \frac{K \cdot N-units}{mbar}$ and $b = 3.379 \times 10^5 \frac{K^2 \cdot N-units}{mbar}$. The change in refractivity is thus,

$$dN = \left(\frac{\partial N}{\partial p}\right)dp + \left(\frac{\partial N}{\partial T}\right)dT + \left(\frac{\partial N}{\partial e}\right)de \, , \tag{6}$$

$$dN = \left(\frac{a}{T}\right)dp - \left(\frac{ap}{T^2} + \frac{2be}{T^3}\right)dT + \left(\frac{b}{T^2}\right)de \, . \tag{7}$$

To understand the sensitivity of the refractivity to the variation in each variable, i.e. the weighting on the refractivity gradient by the atmospheric variables, consider the standard pressure and temperature at 50% relative humidity. In this case, T = 293 K, p = 1013 mbar, and e = 23.4 mbar. The differential refractivity is,

$$dN = 0.265dp - 1.61dT + 4.35de \, . \tag{8}$$

The conditions that result in AP may be estimated for each variable by holding the others constant. Table 2 shows the results. The temperature and humidity gradients are physically realizable.

Table 2 AP Conditions in standard atmosphere

AP Criterion	Description
$\frac{dp}{dh} < -592 \frac{mbar}{km}$	A very sharp pressure decrease

$\frac{dT}{dh} > 97.5 \frac{K}{km}$	A sharp temperature increase
$\frac{de}{dh} < -36 \frac{mbar}{km}$	A significant decrease in water vapor partial pressure

Possibly the most probable atmospheric conditions resulting in AP is the latter one, a significant decrease in relative humidity with altitude. This occurs many times on clear nights when the air near the surface is quite moist and there is a sharp decrease in moisture content with height. This occurs when warm dry air moves over bodies of cool water

The next most likely event is a temperature inversion. A In this scenario, the temperature sharply increases as a function of height, similar to that shown in Figure 3. This will occur on clear nights where the ground cools more quickly than the air above it. Thus, temperature inversions occur quite often in the between late autumn and early spring.

The temperature increases from 10 deg C at about 50 m to about 6 deg C at 500 m at which point it increases again to approximately 13 deg C at 550 m. Thus the temperature inversion occurs between 500 and 600 m with a gradient of 140 K/km. Again, this gradient is sufficiently large to result in AP.

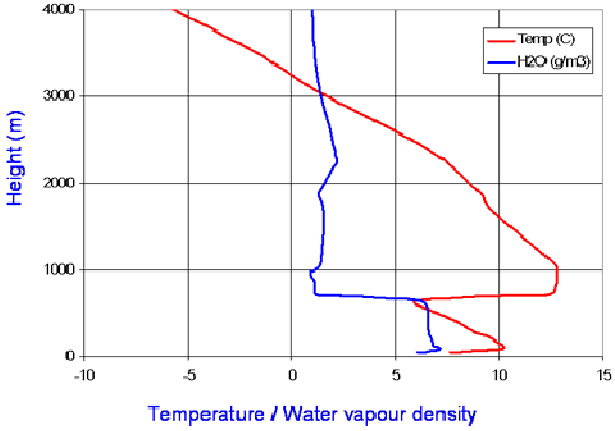

Figure 3 Profile showing temperature inversion. This profile was measured Nov. 7, 2006 over Herstmonceux UK

3. ATMOSPHERIC MEASURING SYSTEMS

The measurement of atmospheric profiles has a long history. Traditionally, the profile is measured directly through the use of radiosondes. More modern techniques include the use of satellite and ground based radiometers to measure the profiles and the delay and modulation superimposed upon GPS signals by the atmospheric effects.

This section briefly summarizes some of the common atmospheric profiling sensors and their associated retrievals.

3.1. Radiosonde Measurements

Radiosonde measurements are the standard to which all other measurement techniques are compared. It is a point measurement, meaning that the measurements are obtained in situ at specific points in the atmosphere at specific times.

A radiosonde is an instrument package to measure the atmospheric variables, temperature, pressure, dew point and relative humidity as a function of altitude. Figure 4 shows a typical radiosonde sensor package.

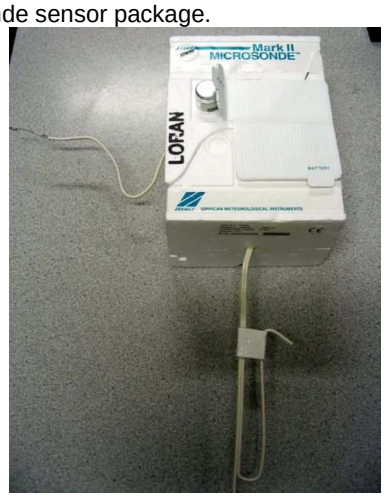

Figure 4 Radiosonde Sensor Package by Sippican

The sensor package contains a number of sensors to measure temperature, pressure, and humidity. It is outfitted with a high altitude balloon to raise it through the atmosphere. As the radiosonde package rises in the atmosphere, it is buffeted by winds at the different atmospheric layers. Thus, it does not rise vertically, but is displaced in the horizontal plane by the wind at the different levels. Modern radiosondes include GPS receivers and transmitters to report its location with GPS precision. Previous systems were tracked optically and via radar to determine its location.

Radiosondes transmit the measured data via radio signals to their base stations. The standard measurement protocol calls for measurements to be reported for standard pressure levels, namely 100, 925, 850, 700, 500, 400, 300, 250, 200, 150, 100, 70, 50, 30, 20, and 10 hPa (Bech, 1998).

In the US, radiosonde measurements are taken at a number of sites across the country at 12 hour intervals, 0000 Z and 1200 Z. Variations in the atmospheric profile between these two time periods are not available from radiosonde measurements. However, NWP fills this gap in the data.

In the situations where the radiosonde data is coincident with the radar data, the data resolution is typically too coarse for the sufficient representation of the refractive environment. For example, the radiosonde profiles from the Peachtree City, Georgia site typically begin data transmission above the inversion layer resulting in AP. Bech et al. (Bech 1998) used radiosonde measurements reported at 10 second intervals to obtain data with sufficient resolution for their AP studies. Finally, the refractive environment is not homogeneous horizontally, i.e. it varies with azimuth and elevation. Therefore, a radiosonde measurement will not give an accurate representation of the three dimensional refractive environment.

3.2. Radiometer Measurements

Radiometers are passive microwave sensing devices. Essentially, they are very sensitive microwave receivers that measure the background temperature. They measure the background noise temperature and relate it back to the

atmospheric measurables through inversion techniques. Figure 5 shows a typical radiometer manufactured by Radiometrics and Figure 6 an associated profile. The temperature profile is from the radiometer and the radiosonde are very close, with the radiometer profile much more continuous. Similarly the humidity profile seems to be a much smoother, continuous profile from the radiometer. The radiosonde measurements tend to oscillate about the radiometer extracted profile, they both follow the same trend.

Figure 5 Radiometer manufactured by Radiometrics.

Satellite based radiometers sense the thermal emission of radiation from space. During scan periods when there is significant cloud cover, the temperatures measured by the radiometers and hence the associated profiles will be biased towards that at the top of the clouds. Similarly, ground based radiometers will have a bias towards the bottom of the clouds.

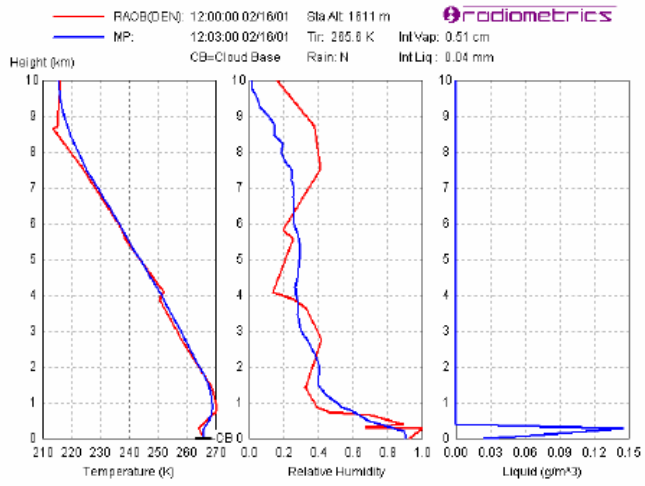

Figure 6 Profile retrieved from the Radiometrics MP3000 radiometer over Boulder Colorado (blue) compared to Denver radiosonde measurements (red) (Ware, 2006).

3.3. Occulting GPS Satellites

A third possibility for profiling the atmosphere is to use occulting GPS satellites as signals of opportunity. Figure 7 shows the geometry of the GPS measurement. One satellite is located near zenith of the receiver while another satellite is beginning to occult, drop below the Earth horizon. The latter signal travels through much more of the atmosphere than the former and as such its signal has more modulation superimposed upon it. The refractive environment distorts the perceived location of the occulting satellite with respect to the true position. As it drops below the horizon, the satellite can be observed due to the atmospheric effects. By knowing the signal characteristics, the exact position of the receiver as well as the true and perceived location of the satellite, the profile can be extracted via model based inversion techniques.

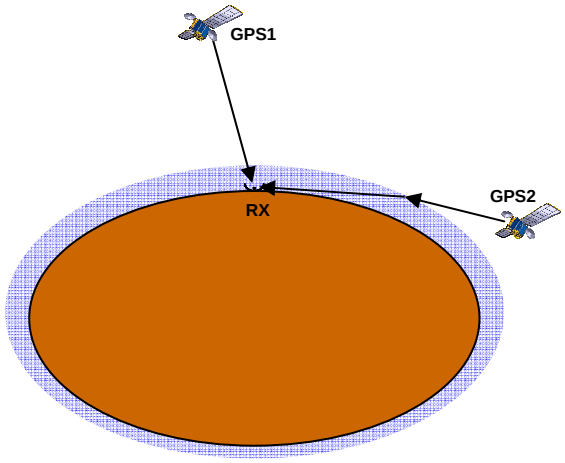

Figure 7 Geometry of using occulting GPS satellites as signals of opportunity.

The TAEM system measures the angle of arrival of the GPS signals and compares that to the expected angle of arrival based upon the actual satellite location. This difference is called the excess bending angle. The TAEM system can use a single receiver to multiple receivers in an array as shown in Figure 8. Using multiple receivers, beamforming is performed to mitigate the multipath effects resulting in a accurate measure of the excess bending angle. This excess bending angle is measured as a function of true angle to the GPS satellite. Figure 9 shows a typical measurement of excess bending angle. There are approximately 30,000 data points collected (cyan and magenta lines). The black lines show this raw data smoothed to an average.

3.3.1. PRA TAEM Data Inversion

Inverting the angle of arrival measurements into an atmospheric profile is performed with a physics based assimilative model.

Physics based assimilative models are physics based simulation programs that assimilate or take in as input measurement data and from the measurement data infers other physical measurable quantities using fundamental physics. Numerical Weather Prediction programs such as MM5 or Weather Research and Forecasting (WRF) model are examples of physics based assimilative models.

The TAEM system utilizes WRF-ARW (Advanced Research WRF). Assimilation and processing modules for the

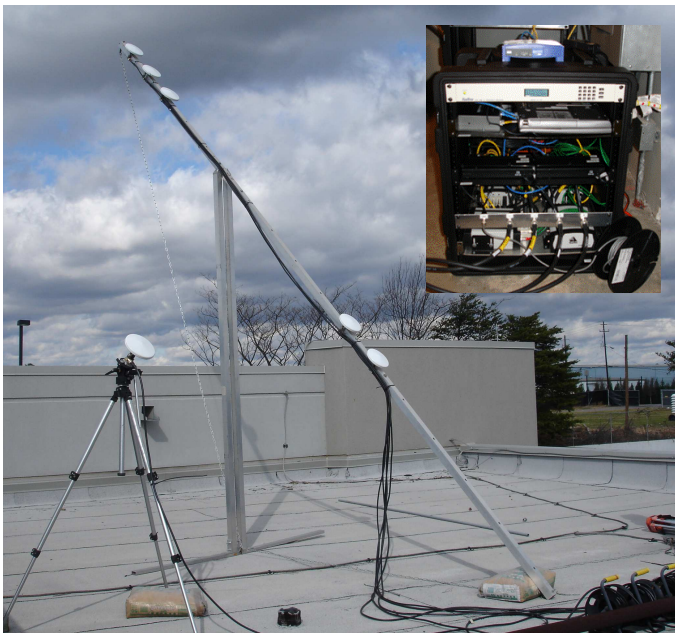

Figure 8 The TAEM antenna and processing system for GPS occultation experiment.

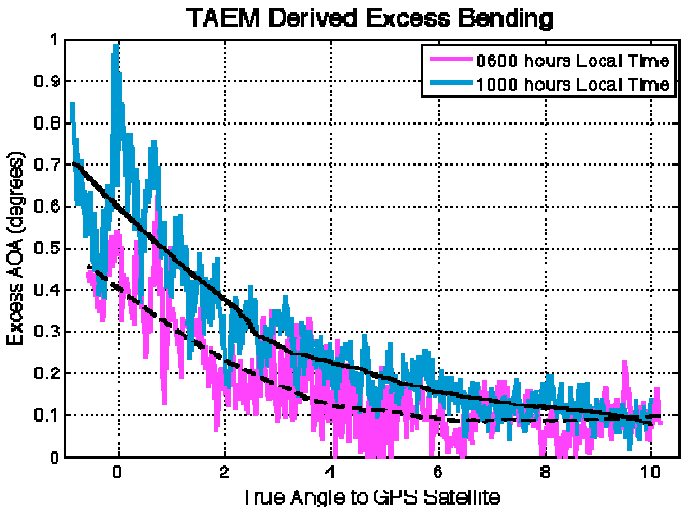

Figure 9 TAEM measured excess angle of arrival.

angle of arrival measurements were created and integrated into the WRF. The modules assimilate the raw angle of arrival measurements from the TAEM measurement system and performs the inversion process. In this manner, the TAEM system can update the WRF data and conversely the 3-D refractivity profile can be extracted from WRF.

4. AP PREDICTION USING TAEM SYSTEM

The prediction of AP using the TAEM uses the data sources to obtain the atmospheric profile in the vicinity of the radar. This profile is then assimilated into WRF to produce a three dimensional characterization of the atmosphere. The refractivity profile is subsequently extracted from WRF and inserted into a propagation modeling routine.

Prediction of low level effects such as AP requires the model to be run with high resolution in the vertical, much higher than typical WRF operation. The pertinent altitudes for AP identification and prediction is less than 2 km, and many times in the first few hundred meters. If equal vertical intervals are utilized, it is recommended that the vertical resolution be greater than 50 m, i.e. at most 50 m between levels. A variable resolution implementation may utilize 10 m vertical levels up to 100 m, then 20 m resolution up to 300 m, etc.

4.1. Propagation Modeling

The propagation modeling routine traces the projected rays from the radar site for a particular azimuth and elevation. The propagation modeling uses the standard Parabolic Equation Method (PEM).

PEM was developed in the 1940's for studies of radio waves within the atmosphere (Leontovich, 1946). Assuming azimuthal symmetry or alternatively a very directional antenna is used, Maxwell's equations are reduced to the two dimensional scalar Helmholtz wave equation (Kuttler, 2002),

$$\nabla^2\psi + k^2 n^2 \psi = 0\,, \tag{9}$$

where k is the wavenumber in free space, n is the refractive index, and ψ is the amplitude of the scalar field.

Transforming the Helmholtz equation into polar spherical coordinates,

$$\frac{\partial^2\psi(r,\theta)}{\partial r^2} + \frac{2jk}{R_0}\frac{\partial\psi(r,\theta)}{\partial\theta} + k^2\left[n^2(r,\theta)\frac{R_0^2}{r^2}\right]\psi(r,\theta) = 0\,. \tag{10}$$

where $j=\sqrt{-1}$, and R_0 is the radius of the Earth. The coordinates, (r,θ), are with reference to the initial field (the antenna) and the center of the Earth. Transforming again into Cartesian coordinates (x,z), a parabolic equation is obtained,

$$\frac{\partial^2\psi(x,z)}{\partial z^2} + 2jk\frac{\partial\psi(x,z)}{\partial z} + k^2\left[m^2(x,z)-1\right]\psi(x,z) = 0 \tag{11}$$

where x is the distance along the surface of the Earth $(x = R_0\theta)$ in the direction of propagation, z is the height above the surface of the Earth $(z = r - R_0)$ and m is the modified index of refraction,

$$m^2(x,z) = n^2(x,z) + \frac{2z}{R_0}\,. \tag{12}$$

The parabolic equation is solved by marching over range steps. At each step, the field component at $x+\Delta x$ is estimated from the component at x by the action of three operators, giving the name split step. In particular, the solution to the parabolic equation at $x+\Delta x$ is given by,

$$\psi(x+\Delta x,z) = e^{j\left(\frac{1}{2}k\Delta x\left(m^2-1\right)\right)}F^{-1}\left(e^{-j\left(\frac{1}{2k}p^2\Delta x\right)}F\left(u(x,z)\right)\right), \tag{13}$$

where F represents the Fourier transform, F^{-1} is the inverse Fourier transform, and $p = k \sin\theta$ where θ is the angle of propagation above the horizontal (McArthur, 1991).

The parabolic equation method is very powerful technique for propagation simulations along the Earth's surface. The utility of the PEM modeling extends into that of irregular and rough terrain, allowing such intractable problems to be solved.

4.2. Anomalous Propagation Forecasting

Once the refractivity profile is extracted, the propagation of the electromagnetic waves transmitted by the radar are simulated via the PEM technique. From this propagation model, AP can be predicted.

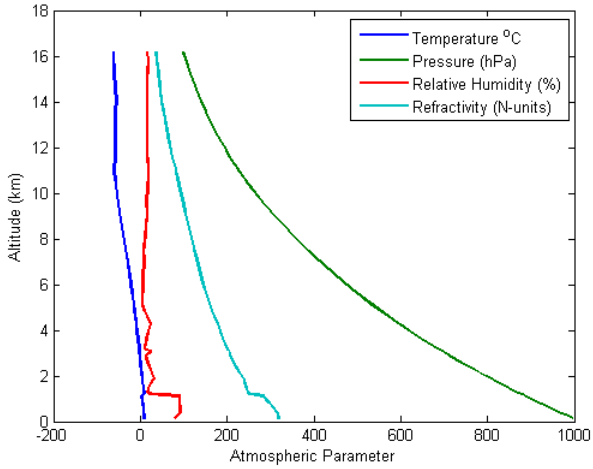

Figure 10 Atmospheric Profile

Consider the atmospheric profile shown in Figure 10. The pressure (green) follows the exponential law with little if any variation. The majority of the variation occurs in the relative humidity (red) which is associated with the water vapor pressure. The refractivity profile (cyan) variations follow the variations in the relative humidity. This relationship is more pronounced in the derivatives of the atmospheric parameters with altitude as shown in Figure 11.

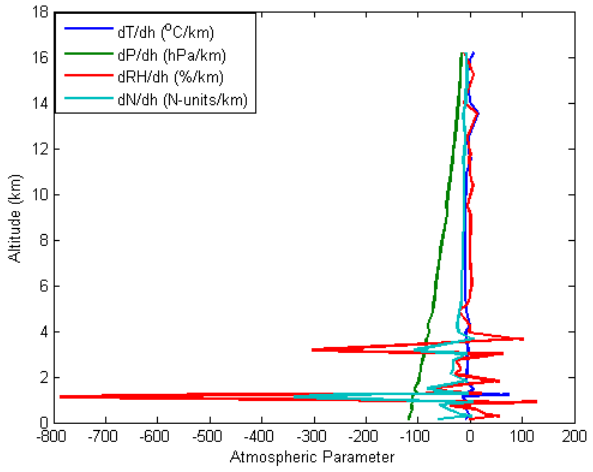

Figure 11 The derivative of the atmospheric parameters with altitude

The relationship is truly pronounced. At approximately 900 m altitude, the humidity drops dramatically as does the refractivity. At approximately 1 km above the surface, the refractivity gradient attains the criteria for anomalous propagation.

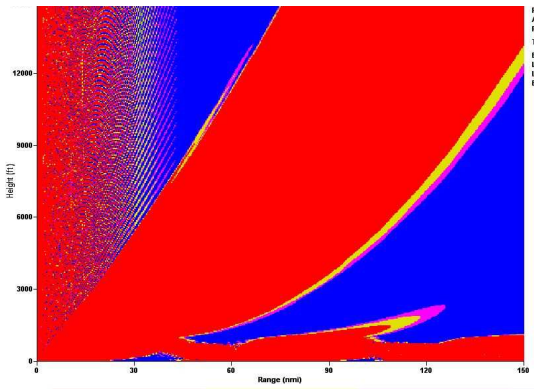

Figure 12 WSR-88D waveform modeled at 0.5 deg elevation for profile shown in Figure 11.

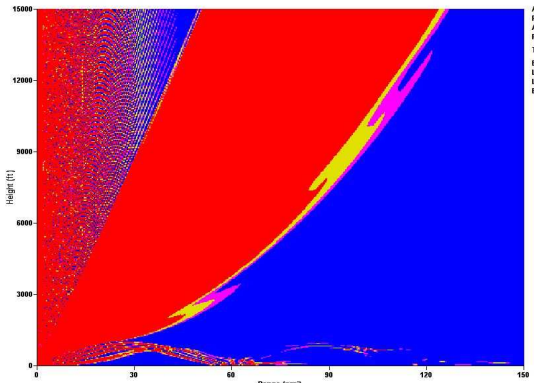

Figure 13 WSR-88D waveform modeled at 1.5 deg.

Figure 12 shows the output of the propagation modeling of a WSR-88D transmitter at 0.5 deg elevation. The expected AP from the decrease in refractivity is observed as a band of signal returning back to the earth along the bottom of the image. However at 1.5 deg elevation the AP does not present itself as seen in Figure 13. Therefore, by modeling several elevations, the minimum elevation required to mitigate AP can be determined. In addition, coupling WRF and PEM (or a WRF PEM module), AP can be forecast for mitigation.

Thus to forecast the AP for all directions, profiles are extracted in 1 degree intervals around the radar site. All 360 profiles are used for input into the PEM routine to obtain the propagation conditions. A "PPI" like display can be created to show the probability of AP.

5. AP AROUND ATLANTA

An evaluation of the AP prediction using TAEM was performed in the Atlanta, Georgia region around the PRA facility. The geography about Atlanta allows for low level

inversion layers and associated surface ducting. Winter and early spring months provide periods of intense ducting phenomena allowing clear identification of infrastructural features such as road and waterways as well as mountain peaks around the city.

The data sources for the evaluation include the Peachtree City Georgia WSR-88D weather radar data as well as the Peachtree City radiosonde measurements. The data was ingested into a version of WRF modified to invert the data and extract the refractivity profiles.

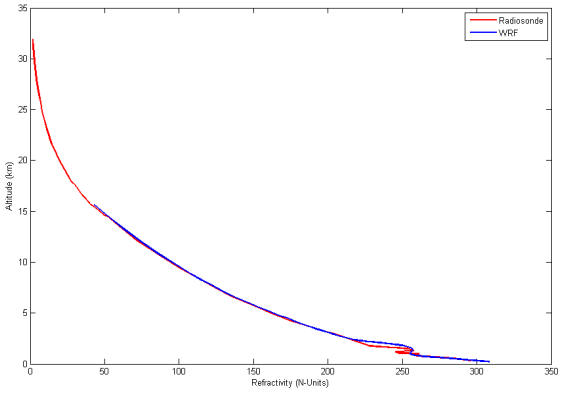

Figure 14 Refractivity profile in Atlanta for May 8, 2007, 1200Z.

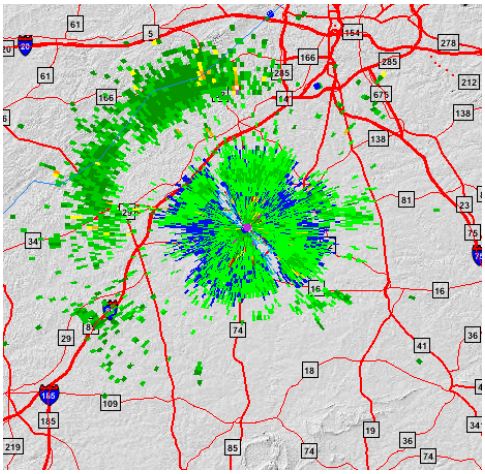

Figure 15 PPI image from Atlanta WSR-88D showing AP at about a 280 to 355 deg azimuth.

Refractivity profiles were extracted directly from radiosonde measurements as well as from WRF. Figure 14 shows the profiles associated from the radiosonde (red) and the profile extracted from WRF (blue). The WRF profile captures the general behavior of the measured profile. Even with the graduated altitude levels in the WRF simulation, WRF was unable to capture the strong gradient required to produce the AP observed at this time period as seen in Figure 15. As a result the propagation model also failed to predict the AP as shown in Figure 16.

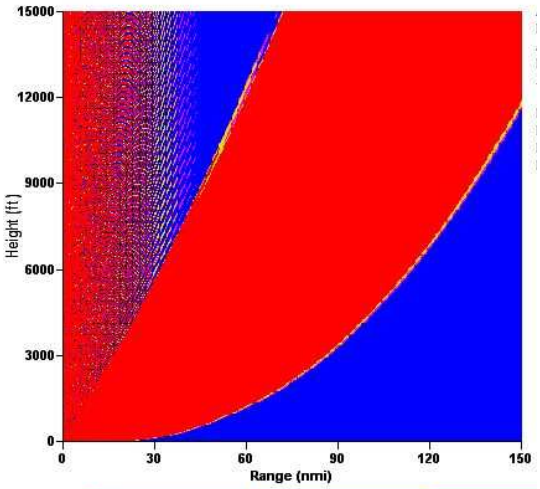

Figure 16 Propagation modeling for Atlanta WSR-88D for May 8, 2007 1200Z

A purely geometric argument places the refractivity gradient producing this AP phenomenon at approximately 100-200 m above the ground, well below the first level recorded by the radiosonde or the WRF model. Therefore it is not surprising that the propagation modeling missed the AP. This is actually very typical in the Atlanta area and presents an issue for predicting AP from radiosonde data.

It is important to note that the AP identified in Figure 15 is *not* azimuthally symmetric around the radar site, rather it is limited in the azimuth. This indicates that the refractivity field is *not* homogeneous in the horizontal layer as is typically assumed with radiosonde measurements. As such radiosonde measurements alone will not provide sufficient measurement resolution to localize the AP.

6. CONCLUSION

The TAEM system uses signals of opportunity (GPS signals) as well as other local meteorological measurements and provides a mechanism for their assimilation into WRF. WRF generates an estimate of the refractivity field for modeling with RF propagation routines using the Parabolic Equation Method (PEM). The RF modeling routines can quantitatively as well as qualitatively predict AP. This realization is the basis of the TAEM AP prediction and mitigation routines.

To evaluate the concept, the WSR-88D waveform was simulated in the propagation modeling routine for a surface ducting environment measured in San Diego, California in February 26, 2002. The gradient in refractivity surpassed the criterion for AP and the associated AP was identified in modeling the WSR-88D at 0.5 deg elevation. Increasing the elevation to 1.5 deg saw nearly complete mitigation of the AP.

Once the concept was validated, it was applied to the propagation environment around the Atlanta WSR-88D site (KFFC). Though AP was identified in the WSR-88D base reflectivity product, neither the profile nor the propagation modeling predicted the AP. As the inversion layer causing the AP fell below the lowest level of the profile and the profile is used for the propagation model, this is not a surprise however identifies a challenge for forecasting AP.

Future work on the TAEM AP prediction and mitigation system will encompass optimizing the vertical level resolution for both radiosonde measurement and NWP calculation. Additional work on the system includes automation, developing a system that generates a refractivity field model and automatically estimates the AP. A final task is the product visualization. The PRA vision for this product is a PPI display identifying the predicted locations of AP georeferenced with the associated radar site. Such a product can be used as a mask to remove AP from the final data product.

7. ACKNOWLEDGEMENTS

This work was partially funded by the Missile Defense Agency under contract W9113M-04-C-0042**.**

8. REFERENCES

Battan, L.J., 1981: Radar Observation of the Atmosphere, University of Chicago Press, pp. 324.

Bean, B.R. and E.J. Dutton, 1966: Radio Meteorology, Department of Commerce, pp. 435.

Bech, J., D. Bebbington, B. Codina, A. Sairouni, and J. Lorente, 1998: *Evaluation of atmospheric anomalous propagation conditions: an application for weather radars*, Proceeding of EUROPTO Conference on Remote Sensing for Agriculture, Ecosystems, and Hydrology, Barcelona, SPAIN, 22 – 24 September.

Doviak, R and D. Zrnic, 1993: Weather Radar, Academic Press, pp. 563.

Kuttler, J.R. and R. Janaswamy, 2002: *Improved Fourier transform methods for solving the parabolic wave equation*, Radio Science, 37, 2.

Leontovich, M. and V. Fock, 1946: *Solution of the problem of propagation of electromagnetic waves along the Earths surface by the method of parabolic equation*, Journal of Physics of the USSR, V. X, 1, pp. 13-24.

McArthur, R.J. and D. H. O. Bebbington, 1991: *Diffraction over simple terrain obstacles by the method of parabolic equations*, Proceedings Seventh International Conference on Antennas and Propagation, 15 – 18 April, York, UK, pp. 824-827.

Millington, S. C. Wang, R. Crocker, R. Seaman, W. Lewi, 2007: *UK Met Office High Resolution Radar Propagation Project*, Bacimo Conference, 6-8 Nov, Boston, MA.

Rinehart, RE., 1991: Radar for Meteorologists, Rinehart Publications, pp. 333.

Sahr, J.D. and F. D. Lind, 1998: *Passive radio remote sensing of the atmosphere using transmitters of opportunity*, Radio Science Bulletin, 284, p.4-7.

Ware, R., P. Herzegh, F. Vandenberghe, J. Vivekanandan, and E. Westwater, 2006: *Ground based radiometric profiling during dynamic weather conditions*, http://www.radiometrics.com/JAOT_06_preprint.pdf